An FPGA-Based Implementation of a Multifunction Environment Sensing Device for Shared Access with Rotating Radars

Zaheer Khan, Janne J. Lehtomäki, Ekram Hossain, Matti Latva-aho, and Alan Marshall

Abstract

To protect radar receivers and to facilitate shared access (SA) in radar bands, regulatory bodies have recommended the use of spectrum monitoring devices called environmental sensing capability (ESC). High-speed and low-cost ESC devices are required to process in real-time the large amount of data (IQ samples) for detection of radar signals and to differentiate them from secondary users (SUs) signals. In this paper, we present a Field Programmable Gate Array (FPGA) based design and implementation of a multifunction ESC device that can detect radar pulses and can also differentiate them from SU signals in microsecond time scales. The proposed ESC device performs the following tasks in parallel: 1) it detects and differentiates between radar and SU signals; 2) measures received signal strength (RSS) from SUs for radar protection; and 3) also measures SUs' airtime utilization (ATU) in a channel which can be used to perform load balancing (based on ATU) of SUs on different channels for efficient access. Detection of signals requires threshold setting. We present a novel minimum-based threshold setting technique which is suitable for real-time operation of energy detectors. We implement a prototype of the proposed ESC device design on a Wireless Open Access Research Platform node which is equipped with a Xilinx FPGA. We evaluate the performance of the implemented device and show that with very high probability (close to 100%) it detects and differentiates between radar and SU signals. Moreover, it also accurately measures the ATU of SUs.

Index Terms

Spectrum measurements, database, spectrum access system, shared spectrum access, ESC devices, temporal sharing, prototype, FPGA, wireless platforms, radars, and 5G.

I. Introduction

The exponential growth in data usage on smart mobile devices, and the continuous need for wireless connectivity for "new things" in the Internet of Things (IoT) is creating unprecedented data rate demand for

Zaheer Khan, Janne J. Lehtomäki, and Matti Latva-aho are with the University of Oulu, Finland; Ekram Hossain is with the University of Manitoba, Canada, and Alan Marshall is with the University of Liverpool, UK

This work is funded by a Digital solutions in sensing and interactions grant from Infotech Oulu.

wireless spectrum. To overcome the challenge of growing traffic demand, regulatory bodies and wireless researchers are currently investigating various solutions. One such solution is to design techniques that enable improved utilization of existing spectral resources. Another solution is to use more spectrum by designing techniques that enable spectrum usage on a shared access (SA) basis in those frequency bands that are currently allocated exclusively to various radar systems [1]. This solution is motivated by the fact that radar systems are allocated a large amount of spectrum below 6 GHz which is well suited for various wireless communication technologies [1]–[3].

Appropriate knowledge of the radio environment allows the design of efficient access algorithms in both currently allocated and new SA spectrum bands. However, wireless networks operate in diverse environments and obtaining appropriate knowledge can be challenging [4]. To address this challenge, researchers have started to study wireless network designs which consist of a distributed infrastructure of detection/measurement devices. For example, use of measurement capable devices (MCDs) for 5G networks have been proposed in [5], where MCDs represent the network elements (e.g., terminals and sensor devices) that perform radio environment measurements. Moreover, regulatory bodies in [6]–[9] have decided to include new sharing tools in which environment sensing capability (ESC) is an essential component for future SA operations in radar bands. ESC is defined in [6]–[9] as a distributed infrastructure of multiple measurement devices used for protection of incumbent radar systems while maximizing secondary spectrum usage.

The design of an ESC device is a relatively new topic and its development is clearly in early stages [9]. For example, [6] states that detection/measurement techniques for ESC are under development. A working demonstration of the implemented ESC device prototype was presented by us in [10]. Different from our demonstration paper in [10], and also different from other works, there are three areas in which this paper makes contributions: 1) We present algorithms for a multifunction ESC device which performs the following tasks in parallel and in real-time: a) it detects the presence of signals and distinguishes between radar and secondary users' (SUs') signals; b) it measures any harmful interference from SUs for incumbent protection; and c) it measures SU airtime utilization (ATU) in a channel which can be used by a SA system to help improve SU spectrum utilization by performing load balancing of SUs based on ATU on different channels. 2) We provide theoretical background to the proposed ESC device algorithms. For example, to detect signals and differentiate between radar and SU signals in real time, it is important to estimate noise level and set an appropriate threshold value. We present theoretical background for a novel minimum-based threshold setting (MTS) technique for energy detectors which can operate in real-time. Unlike existing approaches which require known noise only samples or expensive operations such as sorting [11], the MTS technique does not require known noise-only samples for threshold setting,

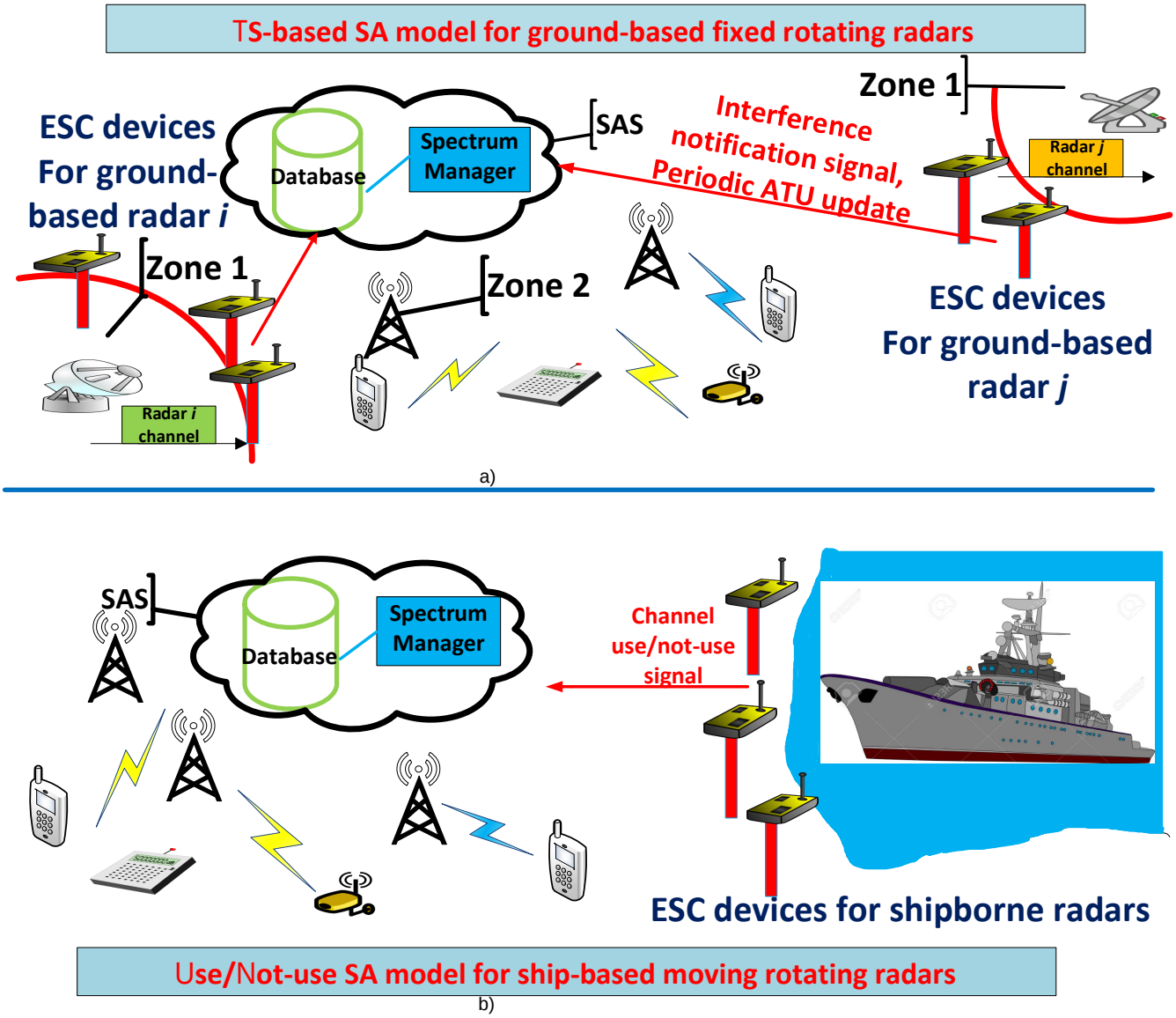

Fig. 1. a) SA model and its functional elements for TS-based SA between wireless communications and ground-based fixed rotating radars; b) SA model and its functional elements for use/not-use SA between wireless communications and ship-borne mobile rotating radars.

instead it estimates the detection threshold from received samples which are unknown combination of signals and noise. 3) We also implement a prototype of the proposed ESC device on a Wireless Open Access Research Platform (WARP) node which is equipped with a Xilinx Virtex Pro Field Programmable Gate Array (FPGA) and an embedded PowerPC processor cores [12]. We provide extensive measurement results that evaluate the real-time performance of the implemented ESC algorithms on the WARP board under various scenarios.

It is important to note that while commercial off the shelf measurement devices, such as spectrum analyzers and signal analyzers, can be used to detect signals, they cannot on their own distinguish between a particular radar's signals and SU signals. To make such commercial off the shelf measurement

devices perform the tasks of ESC devices is both challenging and inefficient in terms of performance, speed and cost. For example, when such a device is used to distinguish between a particular radar's signals and SU signals it requires software-based processing of obtained output samples from an advanced spectrum/signal analyzer. Such software-based processing would incur delays for ESC in terms of decision making. Moreover, an advanced spectrum/signal analyzer in general costs tens of thousands of dollars. A very low-cost prototype solution, such as an RTL-SDR with a cheap single board computer (SBC) and a custom RF front end, would not work because there can be several challenges in real-time implementation of ESC algorithms for SA in radar bands. For example, RTL-SDR is reported to have a stable maximum sampling rate of only 2.4 MS/s which is not enough for sampling radar pulses of microsecond-scale. In contrast, our experiments with WARP platform used sampling rate of 40 MS/s. Also, WARP platform has 14 bit A/D converters as compared to only 8 bit A/D converters with RTL-SDR. Moreover, implementation of proposed ESC algorithms performing multiple functions using host SBC-based processing will lead to processing delays. Note that the proposed FPGA-based ESC device performs such processing tasks in parallel as compared to an RTL-SDR type system which needs processing on a separate PC or a single board computer. Another challenge is that there can be lost samples depending on the interface used between RTL-SDR and the SBC for transferring the samples.

Recently, great efforts have been made to design hardware accelerators to facilitate fast detection systems [13]–[15]. An FPGA-based signal detection and classification system generally offers a flexible solution due to its reconfigurability. Due to these reasons, we propose an FPGA-based ESC device as it can do multiple tasks in parallel while directly processing IQ samples in real-time (with processing speed of several million samples per second). For example, nowadays FPGAs can push the 500MHz performance barrier and have embedded processors, DSP blocks, at ever lower price points. The use of FPGAs for ESC also means that while developing it for a SA system if, for example, some features are required to be modified to take into account a particular radar's and/or SUs signal characteristics all that is required is to reconfigure the FPGA for different signal characteristics.

Although the focus of this paper is to facilitate efficient SA in radar bands, our proposed ESC device algorithms and their implementation can be easily adapted to other spectrum access scenarios. For example, the proposed adaptive noise floor estimation, signal/interference detection and air time utilization measurement algorithms can be easily adapted for use in other wireless network scenarios.

The rest of the paper is organized as follows: First, we present an overview of SA-based models in radar bands, and also provide an overview of the recent incorporation of ESC-based approaches for spectrum sharing. We then present our measurements results and also provide the motivation behind the use of FPGA for implementing the proposed ESC monitoring devices. Then, the proposed ESC design,

its algorithms and their implementation on an FPGA are presented. Before concluding the paper, we also evaluate under various scenarios the performance of the implemented ESC device design.

II. State of the Art for SA in Radars Bands

The opening of TV White Spaces (TVWS) for wireless communications was one of the first initiatives in SA-based wireless systems. As a follow up to the TVWS act, radars bands are now a potential candidate for sharing between wireless communication systems and radar systems [1], [16], [17]. From the perspective of spectrum sharing with radar systems, existing models of sharing can be grouped into two major types:

- Models that propose sharing only in the spatial dimension, such as the geographic exclusion zone (GEZ) and the Dynamic Frequency Selection (DFS) model [1], [18].
- Models that use a combination of database and sensing for radars protection. One example is "channel use/not-use" SA model with shipborne (mobile) radars [8], [9], [19]. Another example of sharing is the "temporal sharing (TS)" model for SA with ground-based fixed rotating radars [20].

Different works and reports have shown that existing GEZ and DFS-based sharing models either do not take into account the real spectrum usage of radar systems or they are excessively conservative and unnecessarily prevent spectrum sharing in the radar bands [1].

For efficient SA, Federal Communications Commission (FCC) has initiated steps to examine the models that can reduce the size of exclusion zone around a radar by using a combination of fixed infrastructure-based ESC devices and database-based access control components [6]–[9]. In [19], a network of ESC devices is proposed for a SA system operating in 3.5 GHz band for two purposes: 1) to facilitate the SA system in ensuring protection from SU interference to an incumbent radar operation; 2) to protect the details of an incumbent military radar's operations. Another work in [9] focuses on a simple notification signal-based ESC sharing framework for shipborne military radars in 3.5 GHz. In this work, the task of ESC is to sense signals, and then infer, based on signal strength, whether the radar receivers located off-shore may be receiving (or are about to receive) interference from the on-shore secondary networks that are in the vicinity of the ESC network. In the case of potential interference, the ESC device sends a trigger signal to the SA system, which is a database and a control/access policy server. A high-level network architecture of SA system based channel use/not-use and TS-based approach is illustrated in Fig. 1.

It is important to note that most of the existing state-of-the-art has focused on presenting high-level network architecture for shared access in radar bands. The existing works have only proposed a description of various functions of ESC sensors. Most of these works are recent patents, such as [19], [21], and technical reports by regulatory bodies, such as [6]–[9]. However, in these patents and reports no ESC

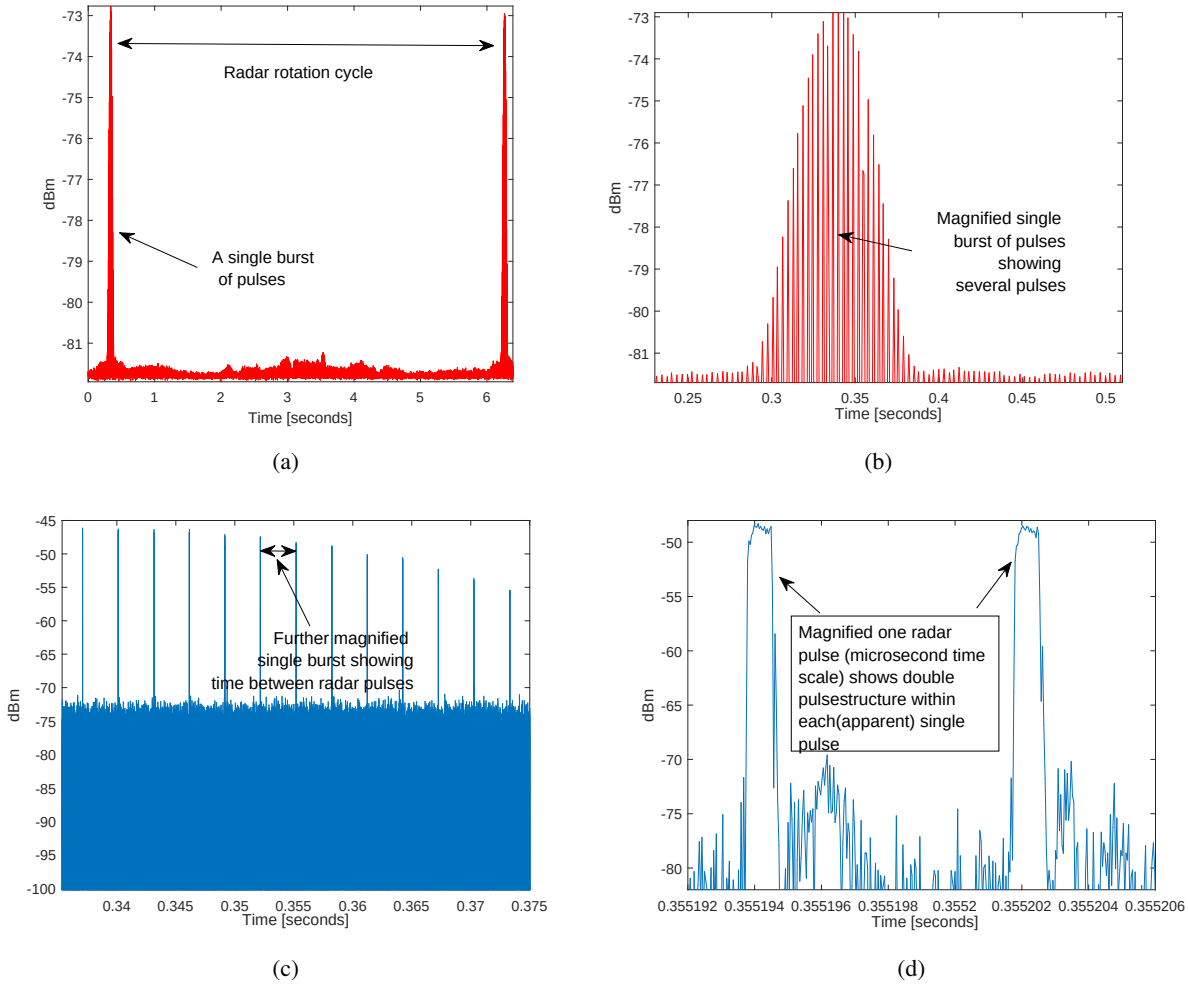

Fig. 2. Example results showing a rotating radars' spectrum usage measurements with different time resolutions. The measured radar is a surveillance radar which operates in 1GHz spectrum near the city of Oulu, Finland.

algorithms or performance results are provided that can be used for comparison purposes. The works in [8] have reported the use of custom made spectrum analyzer device for radar signal detection and its processing with host PC in software. However, no algorithm or performance results are provided in [8] that can be used for comparison.

III. Radar Spectrum Measurement Results and ESC Deployment for SA

A. *Spectrum Measurement Results*

For real-time practical design of an ESC device for shared access (SA) with radar systems, we need to measure radar systems to obtain and understand their various spectrum usage characteristics in different spectrum bands. We ran an extensive measurement campaign in Finland and found that most radar systems currently being utilized below 6 GHz are of rotating radar types. Moreover, currently, rotating radar systems are also the most common ones used for weather and air surveillance in other parts of the world. These

radar systems operate in different spectrum bands, and they have highly directional rotating antennas providing coverage over a large area (e.g., they can have a range of 150-200 km). Details of basic radar principles and operations can be found in [22].

It is possible that in the future rotating radars will be replaced with phased array radar systems. In the case when a rotating radar will be replaced by a phased array radar system our proposed device will still be of benefit for shared access with such a radar system. For example, the proposed real-time adaptive noise floor estimation, signal/interference detection and air time utilization measurement algorithms can be easily adapted for use in SA with a phased radar system.

In our measurement campaign, we measured three different rotating radar systems: 1) a weather radar system in the 5 GHz band; 2) a surveillance radar system in the 1030 MHz uplink channel and its 1090 MHz downlink channel; and 3) a surveillance radar in 2200-2245 MHz band. Measurements were performed with an Agilent N6841A RF sensor connected to a wideband, omnidirectional antenna (ARA CMA-118/A) [22]. The measurements were based on recording continuous (no time domain gaps) stream of IQ samples. Measurements were performed at various locations with respect to a particular radar system and also with various sampling rates. Measurement duration was at least 30 minutes at each location. In Fig. 2a-d, we present examples of high time resolution results showing bursts of pulses of one of the measured radars. Fig. 2a and also our detailed measurement results presented in [23] show that a rotating radar system has a particular duty cycle. It can be seen in Fig. 2a that due to a radar's antenna rotation there are pauses between two bursts (groups) of pulses received from the radar. In particular, results from our measurement campaign show (see [23]) that the pauses between any two group of pulses for the two measured surveillance radars are periodic, with pauses of approximately 3.44 and 5.93 seconds between the group of pulses. The pauses between any two group of pulses for a weather radar are quasi-periodic, with pauses that vary from 13.1 seconds to 21.1 seconds. As proposed in [20], [23], these periodic and quasi-periodic pauses offer the potential of temporally sharing the rotating radar spectrum. For the real-time experiments with WARP platform sampling rate of 40 MS/s was used.

To detect radar signals and to differentiate them from other signals, typically received train of signals is processed and pulses matching some known characteristics of radar are considered as potential radar pulses [24]–[26]. To this end, very high time resolution measurements of received radar signals are required. Fig. 2b shows high time resolution version of single burst of pulses showing several pulses within one burst, and Fig. 2c shows that within any two pulses contained in a single burst there are quiet periods of equal length. Finally, in Fig. 2d we show a single pulse with microsecond time resolution. It can be seen that there is double pulse structure within (apparent) single pulse of the surveillance radar. The duration of one pulse within each double pulse is close to 1 μs. Our proposed method takes such pulse features

into account.

B. Deployment of ESC Devices

The works in [7]–[9] have proposed the deployment of ESC devices along coastal areas for channel use/not-use based SA with shipborne mobile radars. However, the deployment of ESC devices to enable other models of SA, such as TS-based SA with a ground-based fixed radar [20], requires more careful planning. Based on the measured/analyzed features of different ground-based rotating radar systems, we incorporate ESC-assisted sharing in the TS-based model [20] which looks for potential sharing opportunities both in space and time dimensions. In the incorporated model, the area around a rotating radar is divided into three zones, and the three different zones around a radar are modeled as follows:

- At a distance of few kilometres (km) from a rotating radar system a network of sensor devices called ESC are deployed around a radar station. Measurement results in [23], [27], [28] show that within very close distance even the sidelobe signal can be strong enough to interfere with wireless communications. Therefore, it is suitable for both radar systems and wireless communication systems to have a zone of radius approximately 3 to 4 km, where any secondary transmissions are forbidden. We call this zone as exclusion zone or Zone 1.
- In Zone 2, the SU devices exploit temporal sharing every time the radar's main beam is pointing in another direction. In Zone 2 only temporal sharing is allowed in which network is not allowed to transmit during the time when the radar's main beam is pointing to it, and is also not allowed during the guard interval before and after that time period (see Fig. 3). To avoid any possible interference with the side lobes of a radar due to transmissions caused by SUs in Zone 2, when an ESC device detects aggregate received signal strength exceeding a critical threshold value (defined by a regulatory body), it notifies the SA system, which in turn instructs the access points to move some of their users to another channel to avoid any possibility of interference.
- In Zone 3, the users are free to use the spectrum, as due to being at large distances from a radar they are outside the interference area of the radar. This distance needs to be calculated by a regulatory body using extensive measurement campaigns. In general, the starting point for the Zone 3 can vary, depending on the specific site. The work in [1] has suggested it to be between 72 and 121 km from a radar site.

Next, we present details of our proposed ESC device and its algorithms.

IV. Proposed ESC Device for Two Different SA Scenarios

Algorithm 1 describes the main steps for the proposed ESC device under two different sharing scenarios: 1) the channel use/not-use SA; and 2) the TS-based SA, in which SUs outside Zone 1 can communicate

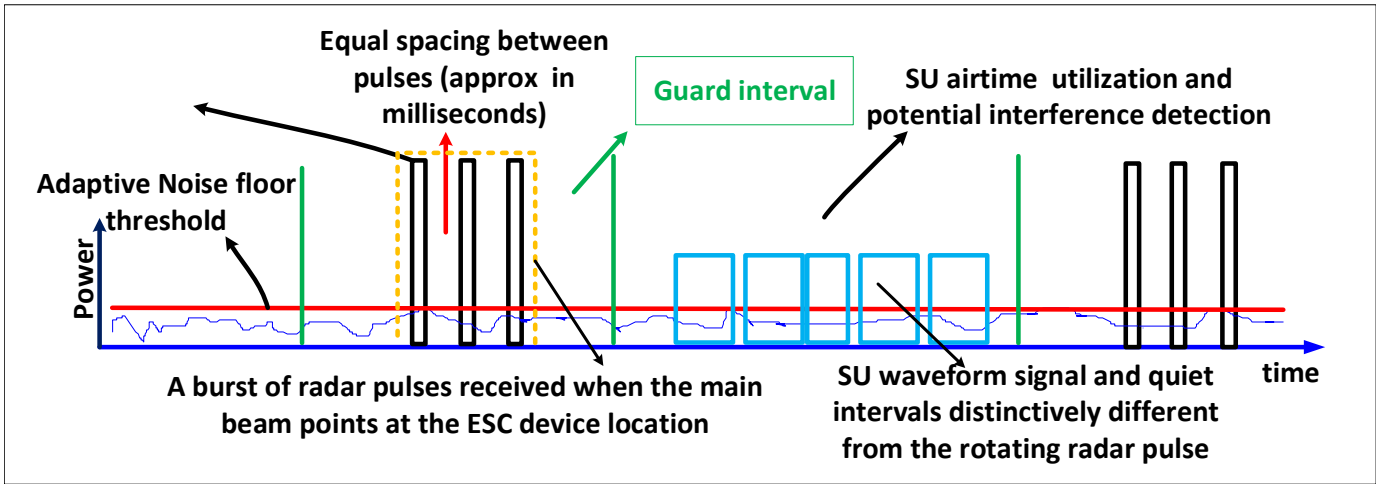

Fig. 3. An example illustrating radar and SU transmissions in TS-based SA.

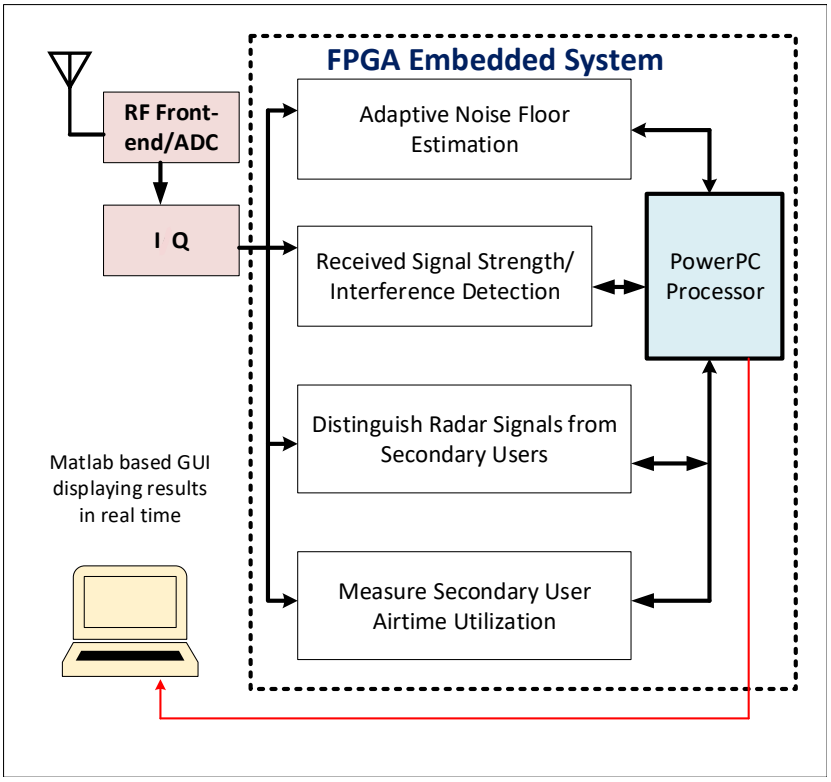

Fig. 4. Block diagram of the main tasks performed by the proposed ESC device.

during the time intervals except when the main beam is pointing in their direction plus the guard intervals before and after the main beam arrival time.

When sharing rules for the radar spectrum are under the use/not-use model then in Algorithm 1 the ESC device performs the following tasks in real-time: it measures/updates the noise level to set a threshold level N_F for signal detection; it analyzes the received signal and measures channel ATU, when radar signals are detected the ESC notifies the SA system to move SUs from the channel; otherwise, it (periodically) notifies the SA system of measured ATU values. However, when sharing rules for the radar spectrum are

Algorithm 1 ESC Device Algorithm for SA with Rotating Radars

```
for Each ESC Device i do
  Initialize: Register with the SA system
  Get sharing rules for the radar system that is to be protected
  if (Sharing Rule == Use/Not-Use) then
    Detect/differentiate between the radar and SU signals.
    if Radar signal is detected then
      Notify the SA system with Not-Use Signal
    else
      Notify the SA system of measured ATU of SUs in a channel.
    end if
  else
    Detect/differentiate between the radar and SU signals.
    if Radar Signal is not detected then
      Compare RSS against protection threshold value
      if RSS > protection threshold value then
        Notify the SA system to move users to other channels or to instruct users to reduce transmissions power levels (as suggested
        by the regulatory body).
      else
        Notify the SA system of measured ATU of SUs in a channel.
      end if
    else
      Measure radar's rotation cycle (arrival time duration between two main beams) and various pulse characteristics (see Table I for
      example).
      Notify the SA system of measured characteristics.
    end if
  end if
end for
```

TABLE I
PULSE CHARACTERISTICS OF THE MEASURED WEATHER RADAR OPERATING IN 5 GHZ NEAR THE CITY OF OULU, FINLAND. PRF DENOTES PULSE REPETITION FREQUENCY

Radar Type	Pulse Spacing in ms	Pulse Duration in μs	Pulse group size
Weather Radar in 5 GHz	$(1/PRF) * 1000 = 1.8$	0.8	(deg/s*360)*PRF=26

under the TS-based model, the ESC device performs the following tasks in real-time: it measures/updates the noise level to set a threshold level N_F for signal detection; it analyzes the received signal, measures received signal strength (RSS) and channel ATU, it determines if the signal exceeding the N_F contains radar signal. When the received signal is not radar signal and it exceeds the interference threshold value I_{th} (defined by a regulatory body), the ESC notifies the SA system to move users from the channel; otherwise, it (periodically) notifies the SA system of measured ATU values. When the received signal is a radar's signal, it measures its rotation cycle (arrival time duration between two main beams) and various pulse characteristics.

Next we explain the details of each of the four tasks performed by the ESC device. The block diagram illustrating the main steps is presented in Fig. 4, and the steps involved in implementation of the ESC device on a WARP board are presented in Fig. 5.

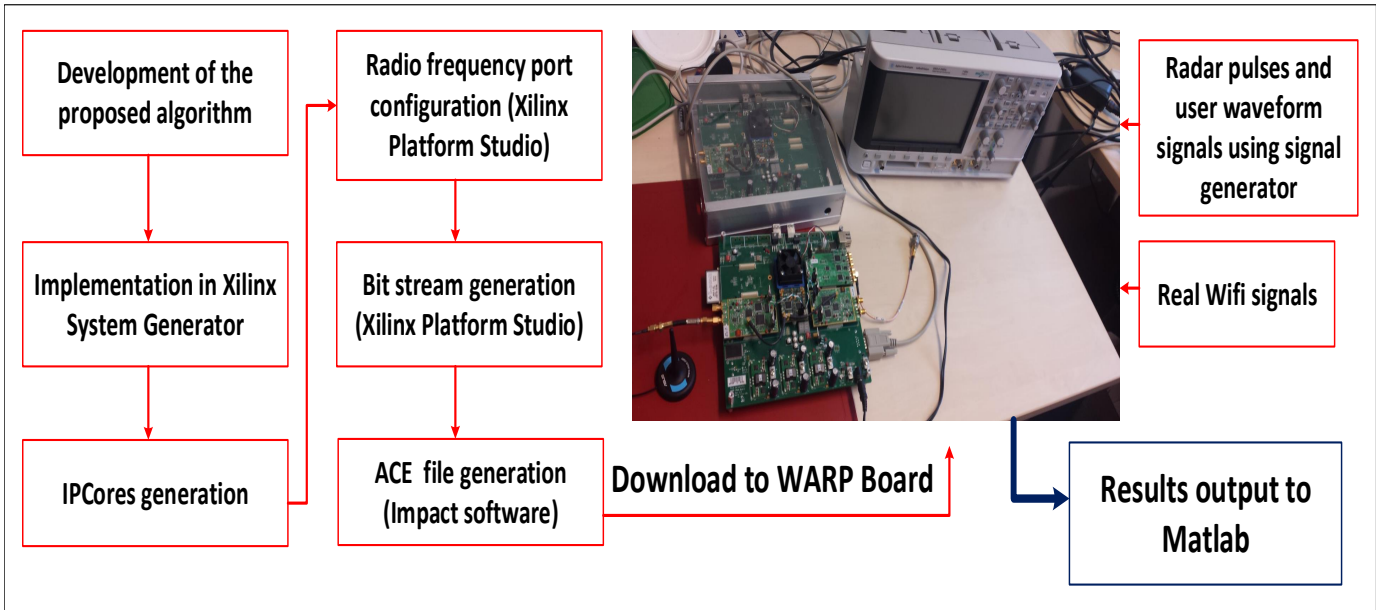

Fig. 5. Steps involved in implementation of the proposed ESC device on a WARP board.

V. Algorithms for Four ESC Tasks and their Implementation Design

In this section, we present a design/prototype of proposed ESC algorithms. It is important to note that there are several challenges in using a typical matched filtering based detection technique for the proposed ESC algorithms. This is due to the reason that matching filtering is mainly a detection technique. Our proposed energy detection based technique not only performs detection of radar pulses but also performs signal classification/differentiation between radar and secondary user signals, detection of harmful interference and also measures secondary user air time utilization. Also, matched filtering has the disadvantage that it can identify only those pulse patterns that have been described in advance. Our proposed technique is not limited in this aspect as it requires only some basic radar pulse characteristics. For example, a rotating radar transmits a narrow beam which consists of a plurality of equally-spaced pulses having a magnitude that is usually significantly greater than magnitude of a SU signal transmitted using a typical unlicensed wireless access scheme. Three basic properties characterize the transmitted beam: 1) pulse repetition frequency (PRF), i.e., the number of pulses of radiation transmitted per second; 2) transmission time, the duration of each pulse; 3) number of pulses received during each time the main beam point towards an ESC device. Moreover, at a given location, the radar pulses are received periodically/quasi-periodically in bursts. As radars are required to listen more than transmit, the received pulses in a burst have distinctive characteristics, such as a short pulse (microsecond-scale) followed by a longer quite period (millisecond-scale). An example of real pulse characteristics (measured by us) of a radar system are given in Table I.

A. Motivation for Implementing the FPGA-Based ESC Device on a WARP Node

FPGAs are currently a suitable option for those applications that require wireless monitoring/measurement systems involving massive and parallel data processing. For example, a recent work in [13] has presented an FPGA-based architecture for managing ultrasonic beacons in a local positioning system. In [29], a real-time FPGA implementation of a spectrum analyzer is presented. The design and test of an FPGA-based radio detection and sensor signal acquisition/processing platform is presented in [30]. The work in [31] presents a design and implementation of an inexpensive nearly all-digital FPGA-based radar receiver.

The most challenging issues in implementing a multifunction ESC device are the speed and accuracy with which large scale IQ samples of received signals are required to be processed in real-time to detect radar pulses and differentiate them from SU signals in microsecond time scales. To address the challenges, we have prototyped the proposed multifunction ESC device design on a WARP node (FPGA board with embedded processor) [12]. At the heart of the proposed ESC design is a Xilinx Virtex-family Pro FPGA and an embedded PowerPC processor cores [12]. This family of FPGAs is very well suited for the real-time DSP-intensive operations required by the proposed multifunction ESC device. For example, a low-cost Xilinx Virtex Pro FPGA with a sampling frequency of 40 MHz can obtain 32 samples of a single radar pulse (out of a single burst of several pulses) whose duration is 0.8μs. An FPGA can process large number of samples in real time to make multiple detection/measurement decisions in parallel. The proposed algorithms are implemented on the WARP FPGA board using the Xilinx system generator (XSG) which provides the possibility of functional simulation even before the compilation of the designed model. XSG provides a set of models (blocks) for several hardware operations that could be implemented on various Xilinx FPGAs. One of the advantages of XSG is the capability of generating IPCores from the implemented design. In Fig. 5, we present the steps involved in the implementation of the ESC device on a WARP board. A block diagram illustrating the four tasks performed by the proposed ESC device is also presented in Fig. 4. Each of the steps involved in the four tasks of the proposed ESC device are also explained in the next subsections. We also present the complete XSG-based designs and their algorithmic details in the subsequent subsections.

B. Adaptive Noise floor Estimation Using Novel MTS-based Technique

To detect signals and differentiate between radar and SU signals in real time, it is important to estimate noise level and set an appropriate threshold value. When received I^2+Q^2 value exceeds the threshold then signal is declared to be present, otherwise, it is declared to be absent. Note that this refers to detection at the sample level, radar signal detection algorithm processing individual sample level detection results

will be introduced later. The threshold setting separates desired signal level versus unwanted noise level. Threshold setting is critical in energy detection, however, most of the previous works have assumed the availability of noise-only samples or wide measurement bandwidth [11]. We present minimum-based threshold setting (MTS) technique which operates in real-time directly on the energy detection outputs which are an unknown combination of signal samples and noise samples. The MTS technique is a practical application of statistical extreme value theory which is a field of statistics dealing with the occurrence and sizes of rare events, be they larger or smaller than usual [32]. Extreme value modeling provides a more robust method of threshold setting when a sufficient amount of $I^2 + Q^2$ samples are available. As an FPGA can obtain/process large number of IQ samples in a fraction of a second the extreme value modelling is particularly suitable for the proposed FPGA-based implementation.

Two different approaches exist for practical extreme value applications [32]. The MTS technique implemented in this work is related to the approach which relies on deriving block maxima (minima) series. In simple words, the MTS technique uses the fact that mostly signal samples are not randomly distributed among all the received samples but are clustered together. For example, samples corresponding to the same packet or same radar pulse are naturally clustered together in time domain. Also, this means that noise-only samples are clustered together. When we use minimum operation, we can aim at finding the energy detector output with noise-only samples. Then this value is used for estimating the noise floor after correcting the bias involved with using the minimum value. Next we provide the theoretical details behind the MTS technique.

Lets' denote the output of energy detector as Y_i, where i is the index number of the output. The statistics of the noise only case for an energy detector output Y_i are described by the chi-squared distribution which is usually denoted by χ^2. The chi-square distribution with K_{AV} degrees of freedom is the distribution of a sum of the squares of K_{AV} independent, normally distributed components. For a digital energy detector, output Y_i has a chi-square distribution with $2K_{AV}$ degrees of freedom, where K_{AV} here is the number of independent signal samples each contributing a vector signal component with normally distributed in-phase and quadrature components which are commonly known as IQ samples. The mean of noise-only energy detector outputs is $\mu = 2K_{AV}$, and the variance is $\sigma^2 = 4K_{AV}$. It is important to note that the distribution of the samples with signal(s) present does not really matter for the proposed MTS technique.

According to Extreme Value Theory, the maximum (minimum) of $X_1, X_2, \cdots, X_N$ standard normal variables converges to the Standard Gumbel extreme value Distribution. It is important to note that dealing with minima follows the same approaches and in applications all needed to be done is to reverse the signs of the observations and apply procedures for maxima as

$$\min\ X_i = -\max\ (-X_i) \tag{1}$$

The mean of the Standard Gumbel extreme value distribution is [32], [33]

$$\begin{aligned}\int_{-\infty}^{+\infty} y\exp(-y)\exp\{-\exp(-(y))\}dy &= -\int_{0}^{+\infty}\ln x\exp\{-x\}dx \quad [x=\exp(-y)]\\ &= -\frac{d}{d\alpha}\int_{0}^{+\infty}x^{\alpha}\exp\{-x\}dx\Big|_{\alpha=0}\\ &= -\frac{d}{d\alpha}\Gamma(\alpha+1)\Big|_{\alpha=0}\\ &= -\acute{\Gamma}(1)\\ &= \gamma\approx 0.57721 \quad \text{Euler constant}\end{aligned} \tag{2}$$

and since

$$\begin{aligned}\int_{-\infty}^{+\infty} y^2\exp(-y)\exp\{-\exp(-(y))\}dy &= -\int_{0}^{+\infty}(\ln x)^2\exp\{-x\}dx \quad [x=\exp(-y)]\\ &= -\frac{d^2}{d\alpha^2}\int_{0}^{+\infty}x^{\alpha}\exp\{-x\}dx\Big|_{\alpha=0}\\ &= -\frac{d^2}{d\alpha^2}\Gamma(\alpha+1)\Big|_{\alpha=0}\\ &= \Gamma^{''}(1),\end{aligned} \tag{3}$$

the variance of the Standard Gumbel extreme value distribution is $\Gamma^{''}(1)-[\acute{\Gamma}(1)]^2=\frac{\pi^2}{6}$. The standard extreme value distribution can be generalized by applying a linear transformation to the standard variable. Suppose that X has the standard Gumbel distribution for maximums discussed above then $-X$ has the standard Gumbel distribution for minimums. More generally, if $\mu_G\in\mathbb{R}$ and $\beta_G\in(0,\infty)$ then $\mu_G+X\beta_G$ has Generalized Gumbel extreme value distribution for maximums with μ_G as location parameter and β_G as scale parameter. The location parameter is given as [32], [33]

$$\mu_G=\Phi^{-1}(1-1/N) \tag{4}$$

and the scale parameter is given as

$$\beta_G=\frac{1}{N\phi(\Phi^{-1}(1-1/N))} \tag{5}$$

where N is the number of random variables, Φ^{-1} is the inverse of the normal cumulative distribution function and ϕ is the probability density function of the normal distribution. Using Eqs. (2) and (3), the moments of X and basic properties of expected value and variance, the expected value μ_Z for the

Generalized Gumbel extreme value distribution is

$$\begin{aligned}\mu_Z &= E(\mu_G + X\beta_G) \\ &= \mu_G + E(X)\beta_G \\ &= \mu_G + \gamma\beta_G\end{aligned} \tag{6}$$

and the variance σ_Z^2 is

$$\begin{aligned}\sigma_Z^2 &= \text{var}(\mu_G + X\beta_G) \\ &= \text{var}(X)\beta_G^2 \\ &= \frac{\pi^2}{6}\beta_G^2\end{aligned} \tag{7}$$

Let Y_m denote the minimum of N normal random variables (each with mean μ and variance σ^2). To model the minimum value, we use the negative of the original values (presented above) as follows [32], [33]

$$\begin{aligned}Y_m &= \min(\sigma X + \mu) \\ &= -\max(\sigma X - \mu) \\ &= -\sigma\max(X) + \mu\end{aligned} \tag{8}$$

We get the mean of Y_m as

$$\mu_Y = -\sigma\mu_Z + \mu \tag{9}$$

and the variance of Y_m as

$$\sigma_Y^2 = \sigma^2\sigma_Z^2 \tag{10}$$

We can now get the offset in decibels relatively to the correct mean μ of the input signal. In other words, the mean μ is the correct noise floor which is the value we are estimating. The ratio of minimum to correct value is Y_m/μ and we find its expected value which is used to compensate the offset of the minimum value.

$$\begin{aligned}\eta_{dB} &= E\left[10\log_{10}\left(\frac{Y_m}{\mu}\right)\right] \\ &\approx 10\log_{10}\left(\frac{-\sigma\mu_Z + \mu}{\mu}\right)\end{aligned} \tag{11}$$

Please note that using Eq. (11) leads to approximation since (unless iterative methods are used) we do not know beforehand the fraction of the energy detector outputs that are noise-only. To evaluate the quality

(a)

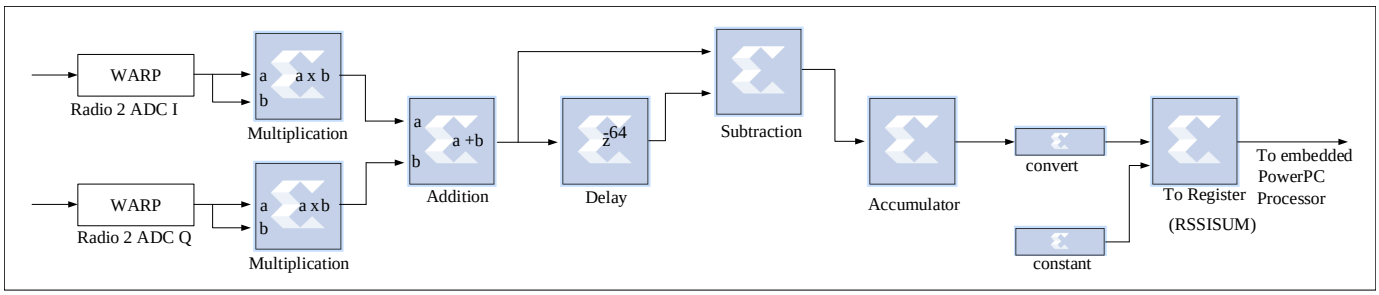

(b)

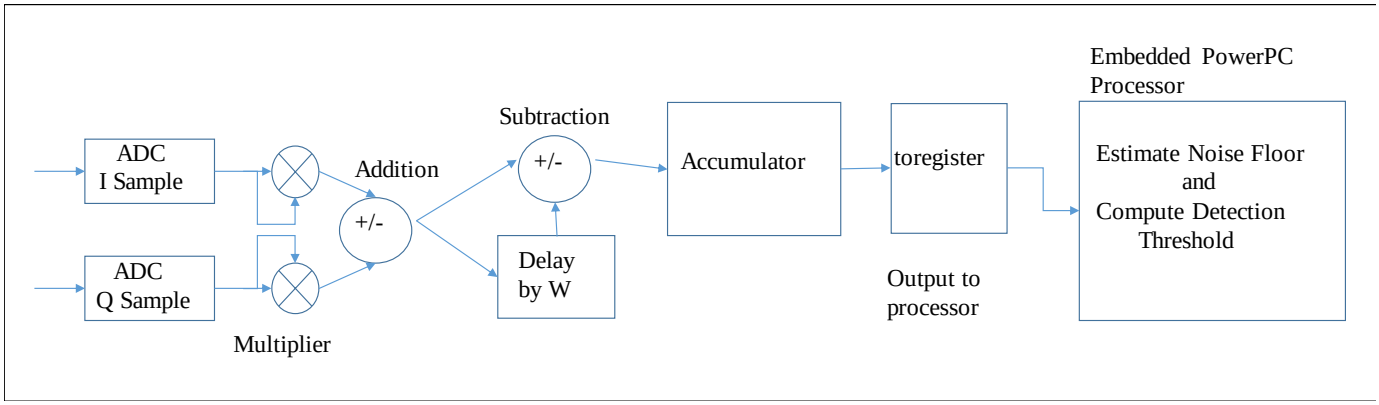

Fig. 6. a) XSG model of the Algorithm 2 for implementation on WARP board; b) Simplified high level block diagram of various components of the implemented model of Algorithm 2.

of estimator the standard deviation is used which in dB scale is

$$\begin{aligned}\sigma_{dB} &= \sqrt{Var\left[\frac{10}{\log_{10} 10}\log_{10} Y_m\right]} \\ &\approx \frac{10}{\log_{10} 10}\sqrt{\sigma_Y^2/\mu_Y^2}\end{aligned} \tag{12}$$

which can be obtained by using the Taylor series expansion of log.

Algorithm 2 Adaptive Noise Floor Estimation (NFE) Algorithm

Input: Moving average window size $W > 0$, moving average $\tilde{S}_m = UINTMAX$ (maximum unsigned integer)
Calculate sum of squared IQ values at instant t, i.e., $S_{m,t} = I_t^2 + Q_t^2$
Wait for the first W values and then obtain moving average at every t: $S_{w,t} = \frac{\sum_{t=(t-W)+1}^{t} S_{m,t}}{W}$
if $\tilde{S}_m > S_{w,t}$ **then**
  Update $\tilde{S}_m = S_{w,t}$
else
  Keep the previous $\tilde{S}_m$
end if
After $R_n >> 0$ updates of $\tilde{S}_m$, output $N_F = \tilde{S}_m - \eta_{dB}$, where η_{dB} is given in Eq. (11) and is used to compensate bias, N_F is the estimated noise floor
For threshold setting T_d, use the obtained N_F and a threshold factor (leading to threshold being m dB above NF).
Repeat the previous steps to get a new update of N_F and T_d.

Implemented Adaptive NFE Module Algorithm: Next we explain how the adaptive NFE module algorithm based on MTS is implemented. The implementation is achieved by calculating the simple moving average S_w (with window size W) of the received of the received squared magnitude of IQ samples, repeating the same process for a large number of times and finally selecting the least value of S_w out of obtained large number of S_w values. The obtained minimum value with the offset Eq. (11) compensated (by subtraction) is the noise floor estimate N_F. Please note that although the offset in Eq. (11) was calculated for the standard chi-squared distribution it is also valid for the scaled chi-squared distribution (for arbitrary variance of the noise-only samples). So we do not need to know the actual noise variance to find the offset, making this method very practical. The noise floor N_F is used to set the detection threshold T_d, as a value m dB above the noise floor. To take into account any changes in the noise floor in real-time, the process is repeated to obtain an updated value of noise floor which is then utilized to update the threshold T_d. Steps involved in adaptive noise floor estimation algorithm are explained in Algorithm 2 and the two block diagrams explaining their XSG-based implementation on WARP board are presented in Fig. 6.

As explained earlier the proposed device exploits the FPGA capability to perform all the main four tasks in parallel. For simplicity, we first explain the interference detection and ATU measurements module and then we explain the radar signal detection module.

C. The Interference detection module

When the ESC device is deployed near a radar which allows TS-based access in Zone 2 then to avoid any interference with the side lobes of a radar from the SUs operating in Zone 2, the proposed ESC device also detects aggregate received signal strength potentially exceeding a critical interference threshold value I_{th} (which is defined by a regulatory body and is given as an input to the ESC device). To detect interference, a simple moving average $S_{w,t}$ (with window size W_I) of the received squared magnitude of IQ samples is compared against the I_{th}. If radar signal is not declared to be present and $S_{w,t} > I_{th}$, a counter is incremented, if radar signal is not declared to be present and $S_{w,t} \leq I_{th}$, the counter is kept the same, otherwise the counter is set to 0 and the values are ignored for the duration equal to the radar burst duration plus the guard interval. For the detection of interference, we need to have a good estimate, so the process comparing $S_{w,t} > I_{th}$ is repeated R_l times, and the interference is declared when the counter value exceeds a pre-defined value. In other words, the counter is used to check how many times $S_{w,t}$ has been greater than I_{th}. To get an update of any potential interference, the previous steps are repeated. Steps involved in Interference Detection Module algorithm are explained in Algorithm 3 and the block diagram explaining their XSG-based implementation on WARP board are presented in Fig. 7.

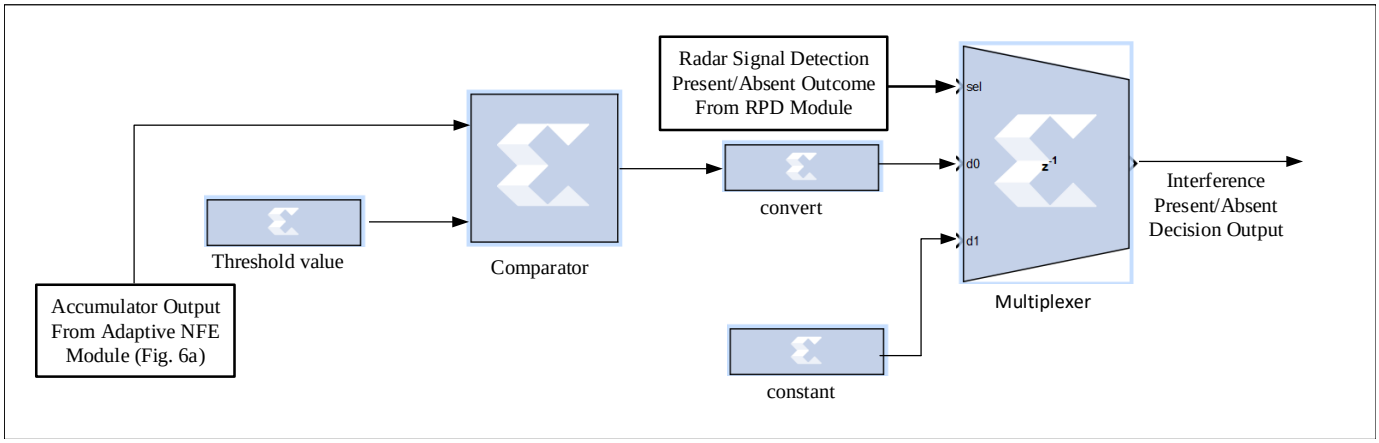

Fig. 7. XSG model of the Algorithm 3 for implementation on WARP board.

Algorithm 3 Interference Detection Module

Input: Interference threshold I_{th}, and comparison counter $C_s = 0$.
Use moving average calculated at every t: $S_{w,t} = \frac{\sum_{t=(t-W_I)+1}^{t} S_{m,t}}{W_I}$
if $(S_{w,t} > I_{th})$ and No radar signal declared **then**
  Update $C_s = C_s + 1$
else if $(S_{w,t} \leq I_{th})$ and No radar signal declared **then**
  Keep the previous C_s
else
  Reset $C_s = 0$
end if
Perform $R_l >> 0$ comparisons of $S_{w,t}$ against I_{th}. Output interference notification to the SA system when $C_s \geq N_I$, where N_I is a design parameter.
Repeat the previous steps to get a new update of whether $C_s \geq N_I$.

D. The airtime utilization (ATU) module

The high speed and parallel-processing capabilities of an FPGA allows us to not only use the ESC device for radar signal detection and interference measurement tasks but also to utilize it for assisting the SA system in terms of better SU spectrum usage. This is achieved by implementing the ATU module on the same device. This module utilizes the estimated noise level by the NFE module. To measure the airtime, the estimated received minimum level is scaled by a factor using Eq. (11) to compensate for bias which is scaled by another factor to set the threshold suitably above the noise floor. The squared magnitude of received IQ sample is compared against the set threshold value. When $S_m > N_F C_s$, a flag C_a is set to 1, otherwise the flag is set to 0. Here design factor C_s includes both bias compensation and a factor to set threshold above noise floor. A simple moving average $S_{a,t}$ (with window size W_a) of C_a values are obtained. For the measurement of airtime, we need to have a good estimate, so the process is repeated R_a times, and the measured airtime is the sum of the R_a values of S_a divided by R_a. The airtime values are output to the SA system only when the radar signal is not detected. The previous steps are repeated to get an updated value. Steps involved in SUs ATU module algorithm are explained

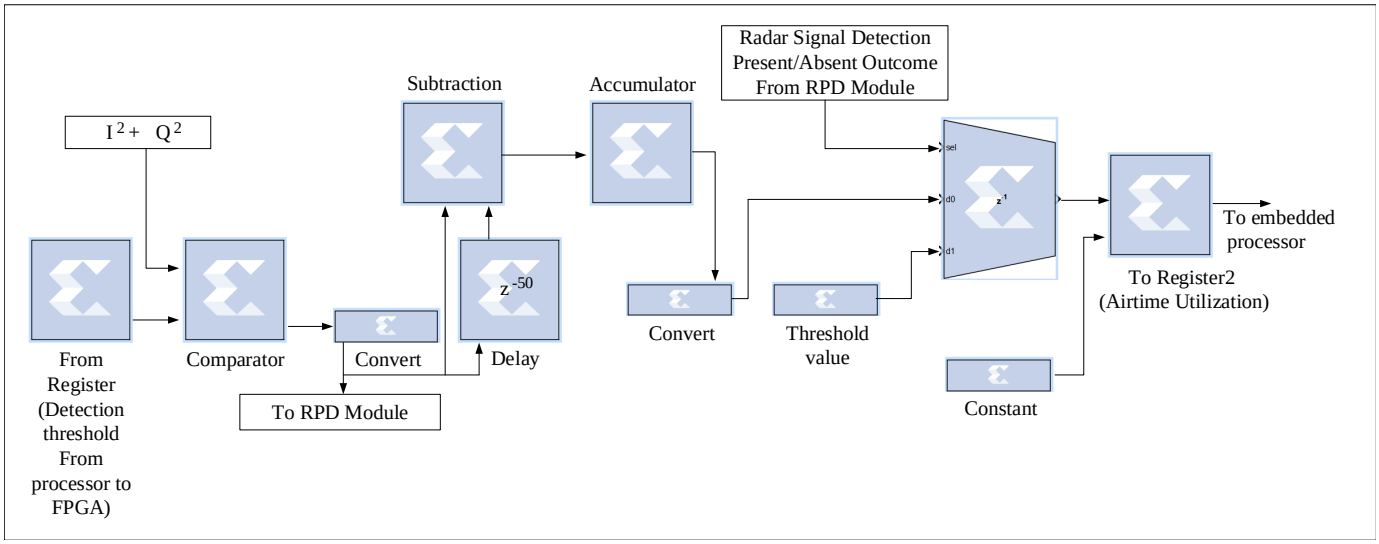

Fig. 8. XSG model of the Algorithm 4 for implementation on WARP board.

in Algorithm 4 and the block diagram explaining their XSG-based implementation on WARP board are presented in Fig. 8.

Algorithm 4 Secondary Users Airtime Utilization Module

Input: Moving average window size $W_a > 0$, scaling factor C_s (a design parameter), and comparison flag $C_a = 0$.
Use $S_{m,t} = I_t^2 + Q_t^2$ and current N_F from NFE module
if $(S_{m,t} > N_F \times C_s)$ **then**
$C_{a,t} = 1$
else
$C_{a,t} = 0$
end if
Obtain moving average at every t: $S_{a,t} = \frac{\sum_{t=(t-W_a)+1}^{t} C_{a,t}}{W_a}$
Obtain $R_a > 0$ samples of $S_{a,t}$, and when radar signal is not declared then output $A_T = \frac{\sum_{t=1}^{R_a} S_{a,t}}{R_a}$, where A_T is the estimated airtime utilization.
Repeat the previous steps to get a new update of A_T.

Radar signal detection module: As illustrated in Fig. 3, over a period of time a radar channel can be occupied by a group of radar pulses at some times and can be occupied by SUs at other times. To obtain accurate estimates of any harmful interference and ATU measurements, it is important to detect radar pulses and also important to distinguish that the measured interference/airtime values are not part of the radar signal. To this end, the ESC device exploits special characteristics of a radar pulse, such as a very short pulse is followed by a longer quiet period. Our proposed technique only requires upper and lower bounds for short pulse duration and long quiet duration between two pulses. When a radar pulse is declared, the measured values of the interference/airtime module are ignored as they are not due to SU transmissions but due to radar signals. The radar pulse detection module uses multiple counters and multiple threshold values to identify a burst of radar pulses which is then declared as radar signal to be present. The parameters for the threshold values are selected based on special characteristics of a radar

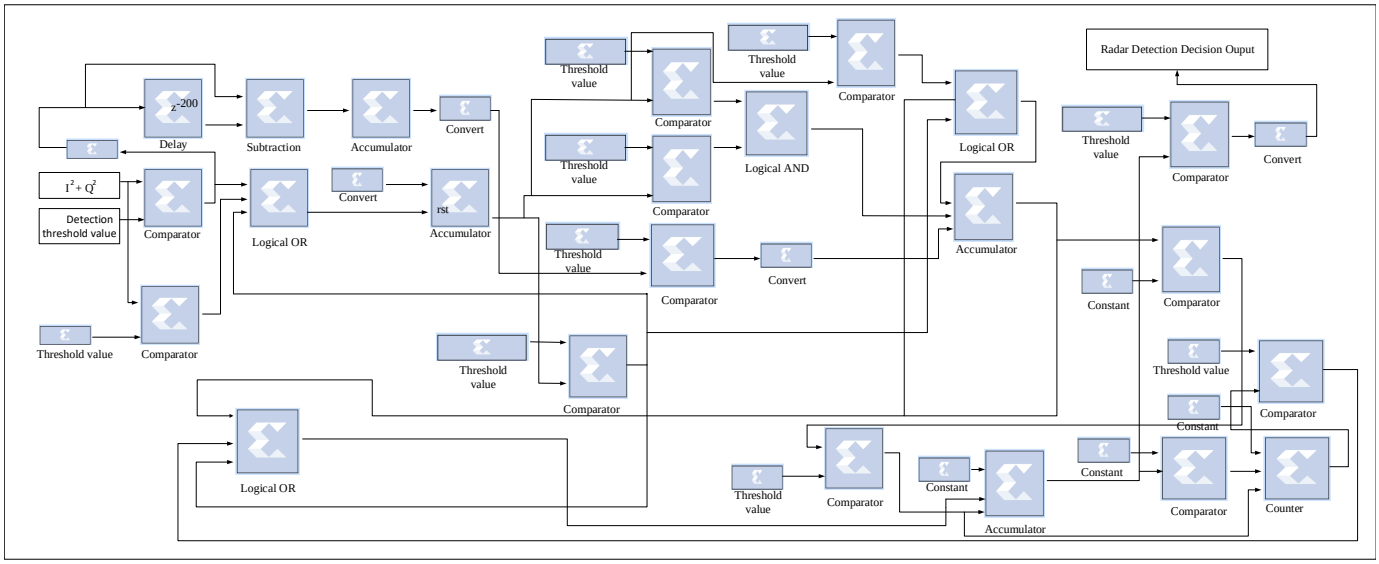

Fig. 9. XSG model of the Algorithm 5 for implementation on WARP board.

Algorithm 5 Radar Pulse Detection (RPD) Module

Input: $C_{a,t}$ values from ATU module, $C_q = 0$, $C_r = 0$, moving average window sizes $W_p, W_q > 0$, and threshold values $T_{p,1}$, $T_{q,1}$ based on radar pulse characteristics.

Signal is Present (Event 1): Simple moving average S_p (with window size W_p) of $C_{a,t}$ values. Increase the counter $C_p = C_p + 1$ when $S_p \geq T_{p,1}$.

Pulse can be Present (Event2): When C_p reaches minδ reset simple moving average S_q (window size W_q) of C_q values to zero. Increase the counter C_q when $C_p \in [min\delta, max\delta]$ and $S_q \geq T_{q,1}$.

if Pulse is present (Event3a): $C_p \in [min\delta, max\delta]$ and C_q reaches a specified constant **then**

Reset $C_p = 0$, $C_q = 0$, a radar pulse is declared, and radar pulse counter is increased $C_r = C_r + 1$.

Declare Radar Signal is Detected: To avoid high false alarms, more than one pulse (out of a burst of pulses) is required to be detected to declare that a radar's signal is present. Radar signal is only detected to be present if C_r reaches a specified number of pulses threshold Th_p. Otherwise the signal is declared to be absent. When radar signal is declared to be present then end of radar signal counter $C_e = C_e + 1$ starting to increment and is reset only when a new pulse is detected.

Declare End of Radar Pulse Train: When radar signal is declared to be present and $C_e \geq Th_e$ then end of radar pulse burst is declared and $C_r = 0$.

else

Pulse is not present (Event3b): When $C_p > max\delta$ before C_q reaches a specified constant then reset $C_p = 0$, $C_q = 0$ and $C_r = 0$

end if

Repeat the previous steps to get new update of detection.

pulse which can be either given as an input to the ESC device or it can be measured itself by the ESC device. The module utilizes the estimated noise level by the NFE module, and the estimated received minimum level scaled by the factor C_s is compared against the squared magnitude of an IQ sample. Whenever $S_{m,t} > N_F C_s$, then it outputs 1, else it outputs 0. Then, a simple moving average of the last W_p samples of outputs is obtained, where W_p is the size of window and is determined by taking the pulse duration into account. The obtained simple moving average is compared against a first threshold value and if it is exceeded then a counter is incremented. When the counter reaches a second threshold value, the algorithm starts looking for the pulse spacing interval by initiating a second simple moving average

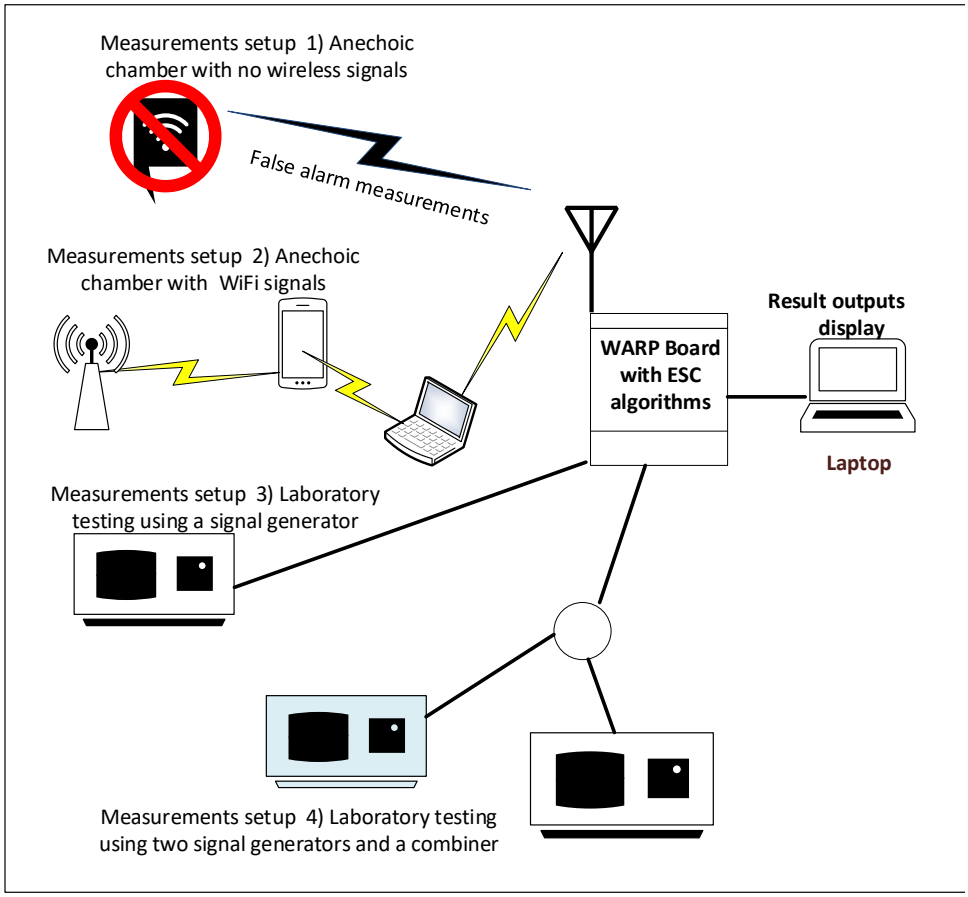

Fig. 10. Illustration of different measurement setups used for performance evaluation and testing of the implemented ESC algorithms on a WARP board.

TABLE II
RESULTS SHOWING AVERAGE OF 100 CHANNEL UTILIZATION OUTPUTS RECORDED FROM THE ESC DEVICE UNDER SIX DIFFERENT TESTING SCENARIOS.

No RF Signals (anechoic chamber)	RF Signals (no user traffic)	File Download (30 MB size)	Skype Audio Call	Skype Video Call	YouTube HD Video
0%	2%	9%	6%	8%	17%

of W_q window size. The size of W_q is determined by taking into account the pulse spacing. When the first counter is not greater than a third threshold value and the pulse spacing interval reaches a fourth threshold, then a short pulse is declared to be present. The previous steps are repeated and if the number of short pulses exceeds a fifth threshold value then it is declared that the radar signal is detected. The previous steps are repeated to get an update. Steps involved in radar signal detection module algorithm are explained in Algorithm 5 and the block diagram explaining their XSG-based implementation on WARP board are presented in Fig. 9.

VI. Performance Evaluation and Discussion

In this section, we evaluate the performance of the ESC algorithms implemented on a WARP board. We evaluate the performance of the implemented algorithms under four different testing setups: 1) anechoic chamber with no RF signals; 2) over the air testing (multiple user transmissions); 3) laboratory testing using a signal generator and 4) receiver blocking testing using multiple signal generators. The four setup scenarios are also illustrated in Fig. 10. In all four testing setups, the WARP board was connected to a laptop computer via serial port. The testing results outputs for display were obtained through the serial port using a terminal program called Putty.

A. Anechoic Chamber Testing

An anechoic chamber is a room that almost completely blocks outside RF signals. We first consider anechoic chamber tests with no RF signals present. These tests can evaluate how often false alarms are generated by the ESC algorithms which are using the proposed MTS noise floor estimation algorithm to set an appropriate threshold value for detection of signals. The anechoic chamber allows us to objectively evaluate the MTS algorithm on the ESC device in terms of its ability to avoid declaring noise as radar or SU signals.

The false alarm measurement tests were performed in the anechoic chamber of the University of Oulu. The anechoic chamber length is 11.5 meters, the width is 6.5 meters and the height is 6.5 meters. The chamber is equipped with 76.7 m^2 conducting ground floor and anechoic wall materials in full compliance with measurement standards. The chamber has frequency range of 30 MHz to 20 GHz.

The ESC device connected to a laptop computer was placed in the anechoic chamber with no RF signals. The device was set to channel 6 (2.437 GHz) of unlicensed band to measure how often signal is found to be present by the device. Table II shows that in the absence of RF signals measured channel airtime utilization is 0%, i.e., the ESC device did not declare signals to be present. This corresponds to 0 false alarm rate. The result shown is the average of 100 recorded outputs from the ESC device. Note that each recorded output represents 10000 signal detection decisions.

B. Over the Air Testing

To test the implemented algorithms in the presence of multiple secondary users, the ESC device connected to a laptop computer was placed in the anechoic room with open door. This allowed RF signals from WiFi/cellular access points to propagate inside the room. In the same room, one HP EliteBook G2 laptop was connected to a Samsung Galaxy S7 smart phone via a WiFi hotspot. The smart phone itself was connected to a WiFi access point. All WiFi connected devices were using channel 6 (2.437 GHz) of

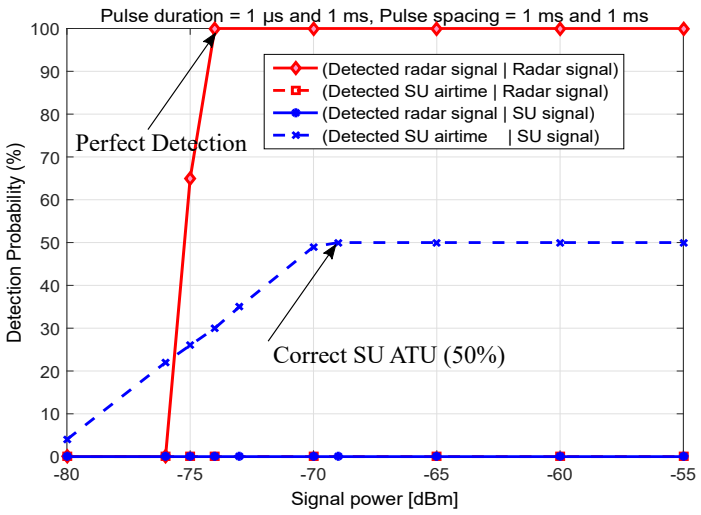

Fig. 11. Performance of the ESC device implemented on the WARP board when radar pulse duration $= 1\mu s$ and pulse spacing $= 1\ ms$, and SU transmission duration $= 1ms$ and silence duration after SU transmission $= 1ms$. Performance is analyzed in terms of radar signal detection and SU ATU estimation.

the unlicensed band. The ESC device was also set to channel 6 of the unlicensed band to measure airtime utilization over the air. The measurement setup is also illustrated in Fig. 10. The result in Table II shows that in the absence of user traffic on smart phones, the measured average airtime was 2 % (which are likely to be beacon signals and other background traffic from the devices). When the smart phone was downloading a 30 MB file size, the measured average airtime was 9 %. The measured average airtime was 6 % for an audio Skype call between the smart phone in the room to the laptop in the room. For a video Skype call between the smart phone and the laptop in the room, the measured average airtime was 8 %. When the smart phone was downloading a high definition (HD) YouTube video the measured average airtime was 17 %. Each of the result shown is the average of 100 recorded outputs from the ESC device. Note that each recorded output represents 10000 signal detection decisions. In none of the cases the device detected users channel utilization as radar signals.

C. Laboratory Testing Using a Signal Generator

Using a signal generator, in our laboratory we evaluated the performance of the implemented ESC device in terms of its accuracy to detect and differentiate between radar and SU signals. We also evaluated its performance in terms airtime utilization of SUs.

For these performance tests, Agilent E4438C vector signal generator was connected to the antenna connector of the WARP board's RF front end running the implemented ESC algorithms. The resulting outputs of the measurements were recorded on a laptop computer via serial port connection between the WARP and the laptop. The signal generator was used to repetitively generate (in real time) a group of radar

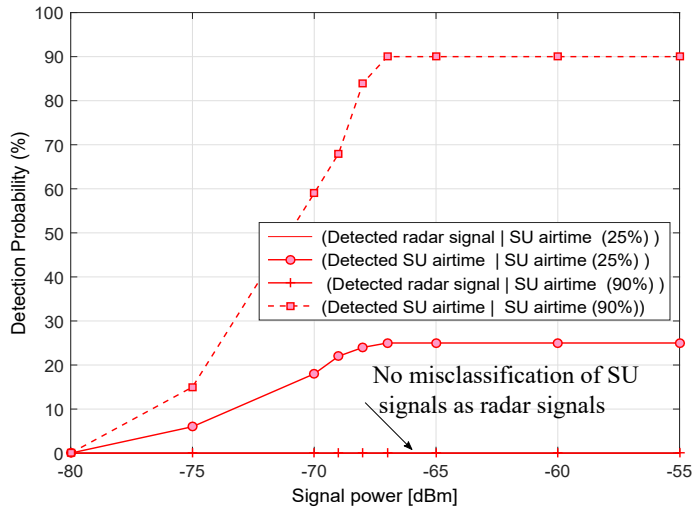

Fig. 12. Performance of the ESC device implemented on the WARP board when SU ATU is varied. Performance is analyzed in terms of signal misclassification and SU ATU estimation.

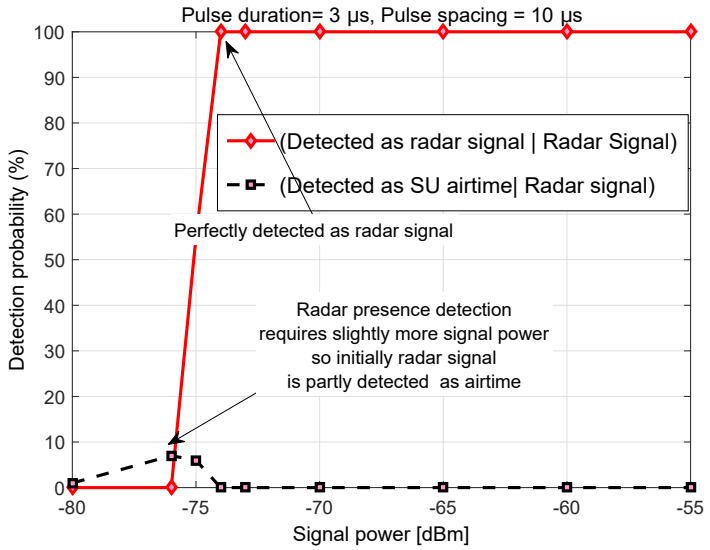

Fig. 13. Performance of the ESC device implemented on the WARP board when radar pulse duration $= 3\mu$s and pulse spacing $= 10$ μs. Performance is analyzed in terms of radar signal detection and signal misclassification.

pulses and SU signals as follows. By setting parameters such as number of radar pulses in a group, pulse width, pulse duration and pulse spacing corresponding to a typical radar pulse, a group of radar pulses were repetitively generated by the signal generator. Similarly, SU signals representing SU transmissions were generated by the signal generator. In other words, the signal generator repetitively generated signals mimicking rotating radar transmissions, such as weather and air surveillance radar transmissions, and also transmissions of SUs.

In Fig. 11, we present detection probability in percentage as a function of signal power in dBm. We

TABLE III
RECEIVER BLOCKING TESTING UNDER WANTED AND UNWANTED OFF-CHANNEL SIGNALS.

Wanted Signal Power	off-channel signal Power (15 MHz offset)	Original airtime utilization of signal of interest	Measured airtime utilization
-50 dBm	-50 dBm	50%	50%
-50 dBm	-40 dBm	50%	50%
-50 dBm	-35 dBm	50%	40%
-50 dBm	-30 dBm	50%	0%
Wanted Signal Power	off-channel signal Power (20 MHz offset)	Original airtime utilization of signal of interest	Measured airtime utilization
-50 dBm	-50 dBm	50%	50%
-50 dBm	-40 dBm	50%	50%
-50 dBm	-35 dBm	50%	50%
-50 dBm	-30 dBm	50%	50%

set pulse duration to be 1 μs for the radar and pulse spacing to be 1 ms for the radar. It can be seen from the figure that, at approximately -75 dBm, the implemented ESC device perfectly detects radar signals. Moreover, it can be seen that the ESC device does not detect radar signals as SU airtime utilization. With 1 ms transmission duration and 1 ms of silent period after each transmission, the SU airtime utilization is 50%. It can be seen from Fig. 11, that the ESC device perfectly detects the airtime utilization at -70 dBm. In Fig. 12, we vary the airtime utilization of an SU by changing its transmission duration and quiet duration interval. We consider two different scenarios where the SU airtime utilization is 25% and 90%, respectively. It can be seen from Fig. 12 that the ESC device never detects SU signals as radar signals, and it perfectly detects the SU airtime utilization of 25% and 90% at -68 dBm.

In Fig. 13, we evaluate the performance of the ESC device under a hypothetical scenario where a radar pulse can also have some airtime by considering a longer pulse duration (3 μs) and a shorter pulse spacing (10 μs). Note that, in reality, radar pulses are of very short duration and their pulse spacing is comparatively very long. It can be seen from the figure that the ESC device at approximately -74 dBm perfectly detects radar signals. Moreover, it can also be seen that, the ESC device does not detect radar signal as SU airtime utilization at -74 dBm and above; however, below -74 dBm radar signal is partly detected as SU airtime. In other words, for the considered scenario, initially radar is classified as non-radar at very low SNR values; however, as the SNR values increase, the ESC device can perfectly detect the received signals.

D. Laboratory Testing for Receiver Blocking

Receiver blocking or desensitisation can occur when a strong off-channel signal appears at the input to a receiver. Next we present performance results for the WARP RF front end relating to its blocking resistance from off-channel signals. For the WARP front end blocking tests, we used an Agilent E4438C

vector signal generator to generate repetitively a signal of interest at 2.437 GHz of unlicensed channel. A Rohde and Schwartz SMIQ06B signal generator was used to generate an off-channel signal. The two generated signals were combined using a combiner Model: ZAPD-4-N+ and given as input to the antenna connector of the WARP board's RF front end running the implemented ESC algorithms. The band of operation for the combiner is 2-4.2 GHz. The resulting outputs of measurements were recorded on a laptop computer via serial port connection between the WARP and the laptop. In Table III, we present receiver blocking testing results as a function of the off-channel signal power in dBm. For the off-channel signal, we consider two different frequency offsets of 15 MHz and 20 MHz, respectively, from the centre frequency 2.437 GHz of the signal of interest. It can be seen that when the off-channel signal amplitude is set to -50 dBm or -40 dBm and there is an offset of 15 MHz, the device can accurately measure the airtime utilization of the signal of interest. This performance degrades when the amplitude of off-channel signal is increased to -35 dBm while the amplitude of the signal of interest is kept the same. When the amplitude of off-channel signal is further increased to -30 dBm then the device suffers from blocking. It can be also seen from Table III that when the frequency offset of the off-channel signal is set to 20 MHz then for the same parameters there is no degradation in airtime measurement performance for the device. It is important to note that the receiver blocking performance for the ESC algorithms can be improved by using RF front end with better blocking-resistance performance.

VII. Conclusion and Future Directions

The regulatory bodies call for the design and deployment of an environmental sensing capability (ESC) system which can assist a shared access (SA) controller to trigger actions for protection of radars from harmful interference, and which also enables efficient SA for secondary users. To protect radar receivers, ESC devices need to detect radar signals and differentiate them from secondary users signals in real time. However, these radar systems have microsecond duration pulses and real-time detection/differentiation of received signals require solutions that are efficient in terms of performance, speed and cost. A low-cost FPGA-based ESC device can offer a flexible monitoring solution due to its reconfigurability and high speed parallel processing capabilities in real-time. In this paper, we present algorithms for an FPGA-based ESC device to monitor the frequency spectrum used by various rotating radar systems, such as fixed ground-based weather radars in the 5 GHz band, and ship-borne mobile rotating radar systems in 3.5 GHz. The proposed design is also implemented on a WARP board with a Xilinx Virtex Pro FPGA. It is shown that as an FPGA-based ESC device can process the received large scale IQ samples in real-time with speed and accuracy, this allows one to design an ESC device with multifunction functionality which can enable both protection of rotating radar receivers and also efficient shared access among secondary users. The performance of the ESC device is tested under various scenarios. The results show that with

very high accuracy the implemented device can 1) detect the presence of a radars' transmissions; 2) measure any interference from SUs for incumbent protection; and 3) measure SU airtime utilization.

One of the extensions we envision for this work is to study the scenarios where a network of implemented FPGA-based ESC monitoring devices are deployed near rotating radar systems and these multiple devices send detection/measurement decisions to an associated SA system network controller to trigger actions. We will use measurement, analytical and simulation based results to assess the impact of processing monitoring data from multiple ESC devices using various decision fusion techniques at the SA system network controller.

REFERENCES

[1] M. Cotton, M. Maior, F. Sanders, E. Nelson, and D. Sicker, "Developing Forward Thinking Rules and Processes to Fully Exploit Spectrum Resources: An Evaluation of Radar Spectrum Use and Management," in *Proceedings of the 12th Annual International Symposium on Advanced Radio Technologies (ISART)*, March, 2012. [Online]. Available: {http://www.its.bldrdoc.gov/publications/2669.aspx}

[2] G. Locke, "An assessment of the near-term viability of accommodating wireless broadband systems in the 1675-1710 MHz, 1755-1780 MHz, 3500-3650 MHz, and 4200-4220 MHz, 4380-4400 MHz bands," National Telecommunications and Information Administration (NTIA), USA, Tech. Rep., October, 2010. [Online]. Available: {http://www.ntia.doc.gov/files/ntia/publications}

[3] V. Ramaswamy and J. T. Correia, "Enabling spectrum sharing between LTE and radar systems in S-Band," in *IEEE Wireless Communications and Networking Conference (WCNC)*, March 2017, pp. 1–6.

[4] M. Bassoli, V. Bianchi, I. D. Munari, and P. Ciampolini, "An IoT approach for an AAL WiFi-based monitoring system," *IEEE Transactions on Instrumentation and Measurement*, vol. Early Access, pp. 1–10, October 2017.

[5] J. Perez-Romero, A. Zalonis, L. Boukhatem, A. Kliks, K. Koutlia, N. Dimitriou, and R. Kurda, "On the use of radio environment maps for interference management in heterogeneous networks," *IEEE Communications Magazine*, vol. 53, no. 8, pp. 184–191, August 2015.

[6] Wireless Innovation Forum, "Requirements for Commercial Operation in the U.S. 3550-3700 MHz Citizens Broadband Radio Service Band," Working Document WINNF-TS-0112, Tech. Rep., 2017. [Online]. Available: {https://workspace.winnforum.org/higherlogic/ws/public/document?document_id=4743&wg_abbrev=SSC&wg_abbrev=SSC}

[7] FCC Committee, "3.5 GHz SAS Conditional Approval Public Notice," Federal Communications Commission, Tech. Rep., 2016.

[8] J. Caulfield, "Proposal to Administer a Environmental Sensing Capability," Key Bridge LLC, USA, Tech. Rep., 2016. [Online]. Available: {https://ecfsapi.fcc.gov/file/60001841831.pdf}

[9] F. H. Sanders, E. F. Drocella, and R. L. Sole, "Using on-shore detected radar signal power for interference protection of off-shore radar receivers," National Telecommunications and Information Administration (NTIA), USA, Tech. Rep., March, 2016. [Online]. Available: {https://www.its.bldrdoc.gov/publications/download/TR-16-521.pdf}

[10] J. J. Lehtomäki, Z. Khan, M. Matinmikko, R. Vuohtoniemi, and A. Marshall, "Demonstration of an environment sensing capability prototype for shared access with rotating radars," in *IEEE International Workshop on Computer-Aided Modeling Analysis and Design of Communication Links and Networks (CAMAD)*, June 2017, pp. 1–2. [Online]. Available: {http://www.ee.oulu.fi/~zaheer/ESCDEMO.pdf}

[11] H. V. Poor, *An Introduction to Signal Detection and Estimation (2Nd Ed.)*. New York, NY, USA: Springer-Verlag New York, Inc., 1994.

[12] Rice University WARP project. [Online]. Available: {http://warp.rice.edu/}

[13] A. Hernández, E. García, D. Gualda, J. M. Villadangos, F. Nombela, and J. Urena, "FPGA-based architecture for managing ultrasonic beacons in a local positioning system," *IEEE Transactions on Instrumentation and Measurement*, vol. 66, no. 8, pp. 1954–1964, Aug 2017.

[14] W. Shi, X. Li, Z. Yu, and G. Overett, "An FPGA-Based hardware accelerator for traffic sign detection," *IEEE Transactions on Very Large Scale Integration (VLSI) Systems*, vol. 25, no. 4, pp. 1362–1372, April 2017.

[15] V. Bhatnagar, G. S. Ouedraogo, M. Gautier, A. Carer, and O. Sentieys, "An FPGA software defined radio platform with a high-level synthesis design flow," in *IEEE 77th Vehicular Technology Conference (VTC Spring)*, June 2013, pp. 1–5.

[16] M. M. Sohul, M. Yao, T. Yang, and J. H. Reed, "Spectrum access system for the citizen broadband radio service," *IEEE Communications Magazine*, vol. 53, no. 7, pp. 18–25, 2015.

[17] M. Ghorbanzadeh, E. Visotsky, P. Moorut, and C. Clancy, "Radar interference into LTE base stations in the 3.5 GHz band," *Physical Communication (Elsevier)*, vol. 20, no. C, pp. 33–47, Sep. 2016.

[18] F. Hessar and S. Roy, "Spectrum sharing between a surveillance radar and secondary WiFi networks," *IEEE Transactions on Aerospace and Electronic Systems*, vol. 52, no. 3, pp. 1434–1448, June 2016.

[19] J. M. Caulfield, "Protecting non-informing incumbent spectrum operations," May 2016. [Online]. Available: https://www.google.com/patents/US9357395

[20] M. Tercero, K. Sung, and J. Zander, "Temporal secondary access opportunities for WLAN in radar bands," in *14th International Symposium on Wireless Personal Multimedia Communications (WPMC)*, October 2011, pp. 1–5.

[21] J. M. Caulfield, "Policy-based protection of non-informing spectrum operations," Dec 2016. [Online]. Available: https://www.google.com/patents/US20160381558

[22] A. Technologies, "Agilent radar measurements," Application Note, Technical Report, Tech. Rep., 2014. [Online]. Available: {http://cp.literature.agilent.com/litweb/pdf/5989-7575EN.pdf}

[23] Z. Khan, J. J. Lehtomaki, S. I. Iellamo, R. Vuohtoniemi, E. Hossain, and Z. Han, "IoT connectivity in radar bands: A shared access model based on spectrum measurements," *IEEE Communications Magazine*, vol. 55, no. 2, pp. 88–96, 2017.

[24] C. J. Hansen, "Radar detection from pulse record with interference," April 2010. [Online]. Available: https://www.google.com/patents/US20050059363

[25] J. M. Belcea, "Method for detection of radar signals," March 2010. [Online]. Available: http://www.google.sr/patents/US20100060508

[26] C. J. Hansen, "Radar detection circuit for a WLAN transceiver," May 2012. [Online]. Available: http://www.google.com/patents/US7593692

[27] E. Drocella, J. Richards, R. Sole, F. Najmy, A. Lundy, and P. McKenna, "3.5 GHz Exclusion Zone Analyses and Methodology," National Telecommunications and Information Administration (NTIA), USA, Tech. Rep., June, 2015. [Online]. Available: {https://www.ntia.doc.gov/report/2015/35-ghz-exclusion-zone-analyses-and-methodology}

[28] F. Paisana, Z. Khan, J. Lehtomäki, L. A. DaSilva, and R. Vuohtoniemi, "Exploring radio environment map architectures for spectrum sharing in the radar bands," in *Proceedings of 23rd International Conference of Telecommunications (ICT)*, 2016, pp. 1–6.

[29] V. Iglesias, J. Grajal, M. A. Sánchez, and M. López-Vallejo, "Implementation of a real-time spectrum analyzer on FPGA platforms," *IEEE Transactions on Instrumentation and Measurement*, vol. 64, no. 2, pp. 338–355, Feb 2015.

[30] S. Saponara and B. Neri, "Radar sensor signal acquisition and multidimensional FFT processing for surveillance applications in transport systems," *IEEE Transactions on Instrumentation and Measurement*, vol. 66, no. 4, pp. 604–615, April 2017.

[31] J. Meier, R. Kelley, B. M. Isom, M. Yeary, and R. D. Palmer, "Leveraging software-defined radio techniques in multichannel digital weather radar receiver design," *IEEE Transactions on Instrumentation and Measurement*, vol. 61, no. 6, pp. 1571–1582, June 2012.

[32] L. de Haan and A. Ferreira, *Extreme Value Theory: An Introduction (Springer Series in Operations Research and Financial Engineering)*. Springer, 2010. [Online]. Available: http://www.amazon.com/Extreme-Value-Theory-Introduction-Engineering/dp/144192020X/ref=sr_1_1?s=books&ie=UTF8&qid=1290511217&sr=1-1

[33] J. Beirlant, Y. Goegebeur, J. Segers, J. Teugels, D. De Waal, and C. Ferro, *Statistics of Extremes: Theory and Applications*, ser. Wiley Series in Probability and Statistics. John Wiley & Sons, 2004. [Online]. Available: https://books.google.fi/books?id=GtIYLAlTcKEC